PROTEIN STRUCTURE REPORT

Crystal structure of human μ-crystallin complexed with NADPH

ZHONGJUN CHENG,[1,2,4] LIHUA SUN,[3,4] JIANHUA HE,[3] AND WEIMIN GONG[1,2]

[1]National Laboratory of Biomacromolecules, Institute of Biophysics, Chinese Academy of Sciences, Beijing 100101, People's Republic of China
[2]School of Life Sciences, University of Science and Technology of China, Hefei, Anhui 230026, People's Republic of China
[3]Shanghai Institute of Applied Physics, Chinese Academy of Sciences, Shanghai 201800, People's Republic of China

(RECEIVED September 12, 2006; FINAL REVISION November 15, 2006; ACCEPTED November 15, 2006)

Abstract

Human cytosolic 3,5,3′-triiodo-L-thyronine-binding protein, also called μ-crystallin or CRYM, plays important physiological roles in transporting 3,5,3′-triiodo-L-thyronine (T_3) into nuclei and regulating thyroid-hormone-related gene expression. The crystal structure of human CRYM's bacterial homolog *Pseudomonas putida* ornithine cyclodeaminase and *Archaeoglobus fulgidus* alanine dehydrogenase have been available, but no CRYM structure has been reported. Here, we report the crystal structure of human CRYM bound with NADPH refined to 2.6 Å, and there is one dimer in the asymmetric unit. The structure contains two domains: a Rossmann fold–like NADPH-binding domain and a dimerization domain. Different conformations of the loop Arg83–His92 have been observed in two monomers of human CRYM in the same asymmetric unit. The peptide bond of Val89–Pro90 is a *trans*-configuration in one monomer but a *cis*-configuration in the other. A detailed comparison of the human μ-crystallin structure with its structurally characterized homologs including the overall comparison and superposition of active sites was conducted. Finally, a putative T_3-binding site in human CRYM is proposed based on comparison with structural homologs.

Keywords: μ-crystallin; p38 cytosolic 3,5,3′-triiodo-L-thyronine-binding protein; crystal structure; *cis*/*trans* isomerization of proline; T_3-binding site; nonsyndromic deafness

Thyroid hormone (TH) plays important regulatory roles in many biological processes through the binding of triiodothyronin (T_3; 3,5,3′-triiodo-L-thyronine) to nuclear receptors α and β, which subsequently alter transcription of specific genes (Zhang and Lazar 2000; Yen 2001). TH is secreted from thyroid gland in the form of thyroxine (T_4; 3,5,3′,5′-tetraiodo-L-thyronine), and most of the T_4 is converted to T_3 by selenium deiodinases (Kohrle 1999). These two forms of TH, after entering the cytoplasm, are transported to the nucleus. Human NADPH-dependent p38 cytosolic T_3-binding protein (p38CTBP) is one of the regulators of TH transportation in cytoplasm, identified by the photoaffinity labeling technique (Hashizume et al. 1986; Beslin et al. 1995). P38CTBP plays an important regulatory role in T_3 transport into the nucleus, and its expression can regulate T_3-related gene expression by changing the cytoplasmic and nuclear distribution of T_3 (Hashizume et al. 1989; Mori et al. 2002).

[4]These authors contributed equally to this work.

Reprint requests to: Weimin Gong, National Laboratory of Biomacromolecules, Institute of Biophysics, Chinese Academy of Sciences, Beijing 100101, P.R. China; e-mail: wgong@ibp.ac.cn; fax: 86-10-64888513; or Jiahua He, Shanghai Institute of Applied Physics, Chinese Academy of Sciences, Shanghai 201800, P.R. China; e-mail: hejh@sinap.ac.cn; fax: 86-21-5955-3021.

Abbreviations: CRYM, μ-crystallin; T_3, 3,5,3′-triiodo-L-thyronine; T_4, 3,5,3′,5′-tetraiodo-L-thyronine; TH, thyroid hormone; P38CTBP, p38 cytosolic 3,5,3′-triiodo-L-thyronine-binding protein; OCD, ornithine cyclodeaminase; AlaDH, alanine dehydrogenase; *Pp*, *Pseudomonas putida*; *Af*, *Archaeoglobus fulgidus.*

Article and publication are at http://www.proteinscience.org/cgi/doi/10.1110/ps.062556907.

Interestingly, microsequencing of four peptides of human p38CTBP revealed that its sequence is identical to that of the human cDNA homolog of kangaroo μ-crystallin (CRYM). CRYM, a taxon-specific 35-kDa protein, is a major structural kangaroo lens protein and is also highly expressed in brain, muscle, and kidney (Wistow and Kim 1991; Kim et al. 1992). Southern blot analysis indicated that a single gene for human CRYM is located on Chromosome 16p (Chen et al. 1992). Although CRYM possesses significant sequence homologies (30%–40%) with two bacterial enzymes, alanine dehydrogenase (AlaDH) and ornithine cyclodeaminase (OCD), CRYM does not show any AlaDH or OCD activities (Kim et al. 1992; Segovia et al. 1997; Schroder et al. 2004). This implies that CRYM could be evolved from a very ancient family of amino-acid-binding proteins.

It has been reported that two mutations, K314T and X315Y (an extension at the C terminus), at the C terminus of CRYM are associated with nonsyndromic deafness in human, and the mutation K314T even loses T_3-binding ability (Abe et al. 2003; Oshima et al. 2006). Although the crystal structures of *Archaeoglobus fulgidus* AlaDH (*Af*AlaDH) and *Pseudomonas putida* OCD (*Pp*OCD) have been solved (Gallagher et al. 2004; Goodman et al. 2004), no CRYM structure is currently available. In order to understand the molecular mechanism of CRYM function, we overexpressed CRYM in *Escherichia coli*, and purified and crystallized this protein. Here, in this study, we report the crystal structure of human CRYM refined to 2.6 Å resolution.

Results and Discussion

Overall structure

The structure of human CRYM was solved using the molecular replacement method with the monomer of a truncated poly(alanine) model of alanine dehydrogenase from *A. fulgidus* (PDB entry 1OMO). There are two monomers in the asymmetric unit with dimensions of ~85 Å × 45 Å × 45 Å (Fig. 1A). The final model includes residues A2–A313, B3–B313, 149 water molecules, and two NADPHs. The last residue Lys314 at the C terminus is invisible, possibly because of its flexibility.

The structure of human CRYM can be divided into two domains: one for dimerization and the other for NADPH binding (Fig. 1A). The dimerization domain, including residues 2–112 and 195–311, folds into a seven-stranded antiparallel sheet, three α-helices, and three 3_{10} helixes. Consistent with the result of Dynamic Light Scattering (DLS) analysis, human CRYM forms a stable dimer by the hydrophobic interface burying 3017 $Å^2$ out of the total 13,400 $Å^2$ accessible surface area per subunit. The residues presented in the hydrophobic interface are mostly located in the β-sheet of the dimerization domain, including Phe7, Val50, Leu59, Val61, Leu72, Leu76, Leu97, Phe99, Leu106, and Val109. Within these residues, most of them are conserved in the CRYM subfamily except Val50, Val61, Leu76, and Val109 (Fig. 2). The NADPH-binding domain, containing residues 113–294, folds into an α/β-fold of Rossmann type. The Rossmann fold, identified in dinucleotide-binding proteins, is also called the mononucleotide-binding motif as it contains a single βαβαβ motif that binds a mononucleotide (Rossmann et al. 1974). The NAD or NADP binding fold contains two Rossmann folds with pseudo-twofold symmetry (Bottoms et al. 2002). The typical Rossmann fold was interrupted by the strand βO and with additional α-helices α8–α10 flanking aside in the human CRYM structure.

The trans/cis *configurations of Pro90*

The two monomers in the asymmetric unit are very similar to the core RMSD of 0.39 Å. However, remarkable differences were observed at the loop between βE and βF (named loop EF). It is intriguing that the conformational changes are associated with the *trans*/*cis* isomerization of Pro90 (Fig. 1B–D). Pro90 in monomer A adopts a *cis*-configuration, while in monomer B it displays a *trans*-configuration. In some cases, the populations of *trans*/*cis* proline isomerization can be characterized by NMR technique to prove the existence of *trans*/*cis* equilibrium (Truckses et al. 1996). Yet no crystal structure has been reported thus far exhibiting Xxx-Pro heterogeneities with both *trans*- and *cis*-proline peptide bonds. There is substantial evidence that this isomerization may play an important role in protein functions (Langsetmo et al. 1989; Ondo-Mbele et al. 2005). In human CRYM, loop EF is not involved in dimerization but is close to the ligand-binding pocket. The conformations of loop EF are also quite different from those in CRYM structural homologs *Af*AlaDH and *Pp*OCD. The high B-factors of loop EF imply that this loop is very flexible and conformational changes may be taken upon the ligand binding (Fig. 1A). Whether the *trans/cis* isomerization of Pro90 in human CRYM plays a biological role or not remains to be further investigated.

NADPH binding

One NADPH molecule was observed in each human CYRM monomer. The main hydrogen bonds of NADPH binding are depicted in Figure 1E. The nicotinamide ring is in *syn* conformation, while the adenine is in *anti* conformation. The adenine moiety shows no direct hydrogen-bonding to the protein except a water molecule that bridges N3 of the adenine base and Asn68. The latter residue also forms a hydrogen bond to the 3′-hydroxyl

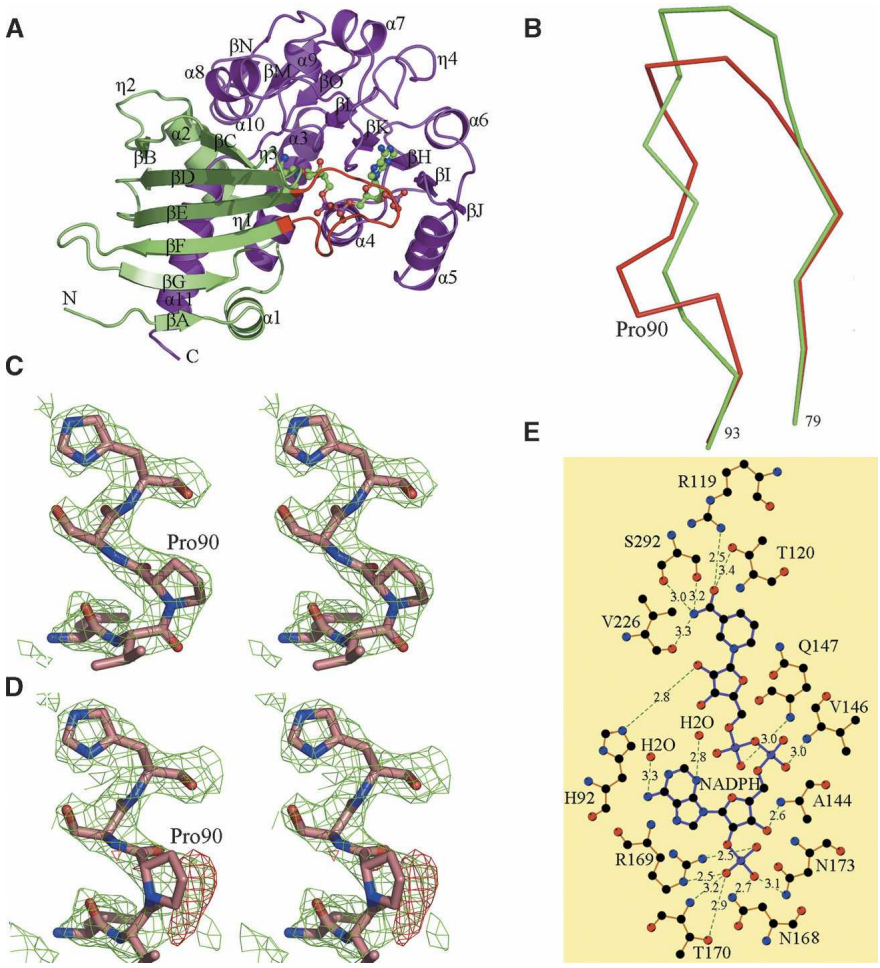

Figure 1. (*A*) The monomer of human CRYM. The dimerization domain is green, while the NADPH binding domain is in magenta. The NADPH molecule is shown in the ball-and-stick model. Loop EF containing Pro90 (residues 80–92) is red. (*B*) Ribbon representation of the overlaid loop EF of the two monomers. The loop with *cis*-Pro90 is red, while the loop with *trans*-Pro90 is blue. (*C*,*D*) The stereoviews of the 1σ $2F_o - F_c$ (green), 3σ $F_o - F_c$ (red) maps of the *cis*-Pro90 refined as *cis*-proline and *trans*-proline, respectively. (*E*) NADPH hydrogen-binding network with human CRYM. Figures 1A–D and 3 were produced by PyMOL (DeLano 2002) and Figure 1E by LIGPLOT (Wallace et al. 1995).

group of the adenosine ribose. The adenine plane faces the side chain of Arg169 whose guanidinium is hydrogen-bonded to the terminal oxygen atoms of the 2′-phosphate on the adenosine ribose. It is often observed in many NADPH-binding proteins that an arginine side chain is parallel to the adenine plane (Carugo and Argos 1997). This type of interaction may have dual functions: its aliphatic chain is able to make hydrophobic interactions and the guanidinium group participates in electrostatic interactions (Carugo and Argos 1997). The side chain of Arg169 is stabilized in place by a salt bridge with the acidic residue Asp82. Besides, Arg169, Asn168, Thr170, and Asn173 also form hydrogen bonds to the 2′-phosphate group of the adenosine ribose.

Human CRYM binds to the pyrophosphoryl moiety of the dinucleotide via a glycine-rich fingerprint region GAGVQA (residues 143–148). The main chain nitrogen atoms of Val146 and Gln147 form hydrogen bonds with two diphosphate oxygen atoms. The nicotinamide moiety forms hydrogen bonds with several residues including Arg119, Ser292, His92, and Val226. His92 interacts with the 3′-hydroxyl group of nicotinamide ribose. The nicotinamide is further stabilized by the hydrogen bonds between its amide group and Arg119, Ser292, and Val226.

Structural comparison with ornithine cycloaminase and alanine dehydrogenase

Although human CRYM has a completely different biological function from OCD and AlaDH, its overall structure is quite similar to *P. putida* OCD (*Pp*OCD, PDB entry 1X7D) and *A. fulgidus* AlaDH (*Af*AlaDH, PDB entry

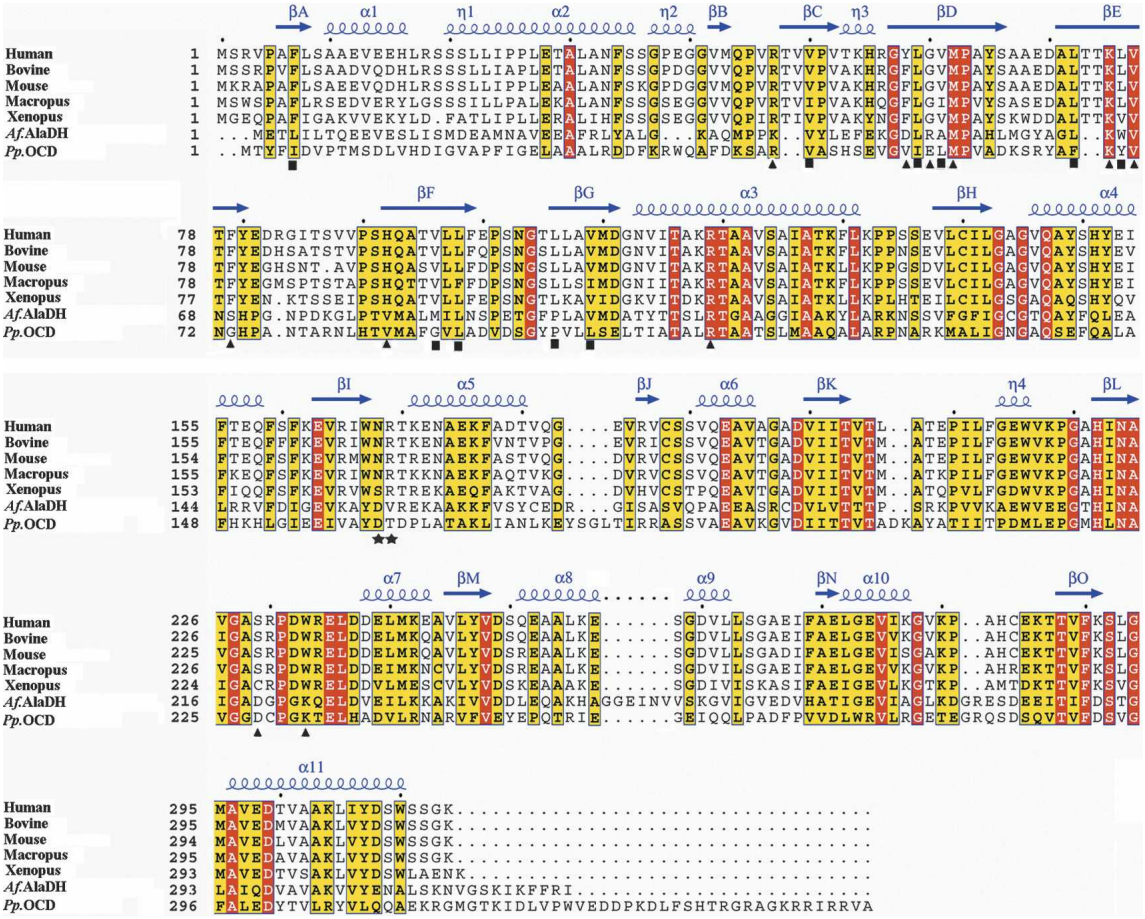

Figure 2. The sequence alignment of CRYMs of *Homo sapiens* (human), *Bos taurus* (bovine), *Mus musculus* (mouse), *Macropus fuliginosus* (Western gray kangaroo), and *Xenopus laevis* (African clawed frog), and OCD from *Archaeoglobus fulgidus* and AlaDH from *Pseudomonas putida*. The sequence accession numbers of the SWISS-PROT database are Q14894, Q2KHX6, O54983, Q28488, Q66KY1, O28608, and Q88H32, respectively. The secondary structures of human CRYM, which is defined by analysis of the structure using the DSSP program (Kabsch and Sander 1983), are indicated above the alignment. Identical residues are labeled in red and similar residues in yellow. Residues involved in putative T_3 binding and hydrophobic dimerization interactions are indicated by black triangles and squares, respectively. Asn168 and Arg169, which function to discriminate NADPH from NADH, are indicated with stars. This sequence alignment is produced by ClustalW (Thompson et al. 1994) and ESPript (Gouet et al. 1999).

1OMO) with the C_α RMSD of 1.6 Å when superimposing the core structures. These three proteins all exist in solution as stable dimers, and a similar dimerization mode has been observed in their crystal structures.

Human CRYM, *Pp*OCD, and *Af*AlaDH all have the nucleotide-binding sequence motif GXGXXG/A, but human CRYM evolved to bind NADPH while the other two proteins bind to NAD^+. NAD is always used as an oxidant in the oxidative degradations, and NADP usually behaves as a reductant in the reactions of reductive biosynthesis with few exceptions (Carugo and Argos 1997). In the crystal structures, these three proteins bind NAD (NADPH) in a similar way except that NADPH has an additional 2′-phosphate group. The discrimination between NAD and NADPH is conducted by residues Asn168 and Arg169 in human CRYM (Fig. 1E), while those two residues are substituted by Asp and Val/Thr in *Pp*OCD and *Af*AlaDH (Fig. 2), in which the negative-charged Asp may prevent the binding of NADP(H).

Superimposing the active site residues of human CRYM, *Pp*OCD, and *Af*AlaDH may shed light on the functional variation of these three proteins. In *Pp*OCD, the α-amino group of ornithine is hydrogen-bonded to Asp228, which is substituted by Ser229 in human CRYM. The δ-amino group is fitted in the hydrophilic pocket, which is destroyed by the following substitution in human CRYM: Glu56 to Gly60, and Lys232 to Trp233. The substitutions of Gly73 by Phe79 and Val85 by His92 in human CRYM make the space too crowded to directly accommodate the ornithine binding. During the transformation from L-ornithine to L-proline, Asp228 and Glu56 play important roles in the proton transfer

(Goodman et al. 2004), yet they are replaced by Ser and Gly in human CRYM.

The active site comparison with *Af*AlaDH reveals that active residues Arg108, Lys65, and Met54 are conserved, while Lys41 and Arg52 are replaced by Arg47 and Gly60 in human CRYM (Fig. 2). As a consequence, two conserved and catalytically important water molecules in the *Af*AlaDH active site were not observed in human CRYM. Furthermore, the enzymatic cofactor NAD^+ in *Af*AlaDH takes the role of a hydride acceptor, while the cofactor NADPH in the human CRYM cannot.

The putative T_3 binding site

In comparison of the human CRYM active site with those of *Af*AlaDH and *Pp*OCD (Gallagher et al. 2004; Goodman et al. 2004), the thyroid hormone T_3-binding site is proposed. The fact that the T_3-binding capacity of human CRYM is regulated by the cofactor NADPH (Vie et al. 1997) suggests that the T_3-binding site should be close to the NADPH molecule or structural changes should be triggered upon NADPH binding.

The T_3 molecule is a modified iodinated tyrosine and shares a common carboxylate moiety with ornithine. In *Pp*OCD, the residues that make contacts with the carboxylate moiety of ornithine are Arg45, Lys69, and Arg112 (Fig. 3A). These three residues are strictly conserved in CRYM (Arg47, Lys75, and Arg119 in human CRYM). Therefore, the carboxylate moiety of T_3 may form salt-bridge interactions with Arg47, Lys75, and Arg119 as in *Pp*OCD (Fig. 3B). If this binding were true, the aromatic side chain of T_3 could fit in the hydrophobic cavity formed by four CRYM specific residues—Phe79, His92, Leu206, and Trp233—which are highly conserved within the CRYM subfamily except that Leu206 is replaced by a methionine in other proteins.

By cDNA microarray analysis, Abe et al. (2003) identified two mutations K314T and X315Y of human CRYM to be associated with nonsyndromic deafness, and both of these mutations caused the aberrant subcellular localization of the protein. It was reported recently that mutation K314T decreased while X315Y increased the T_3-binding affinity (Oshima et al. 2006). However, these two residues are at the very end of the protein, and Lys314 is disordered in our structure probably because of its flexibility. The C terminus is ~30 Å away from the NADPH-binding site. It is unlikely that the C terminus could be directly involved in T_3 binding. The change in the T_3-binding abilities of these two mutations might be a result of altered protein stability, which certainly requires further investigation.

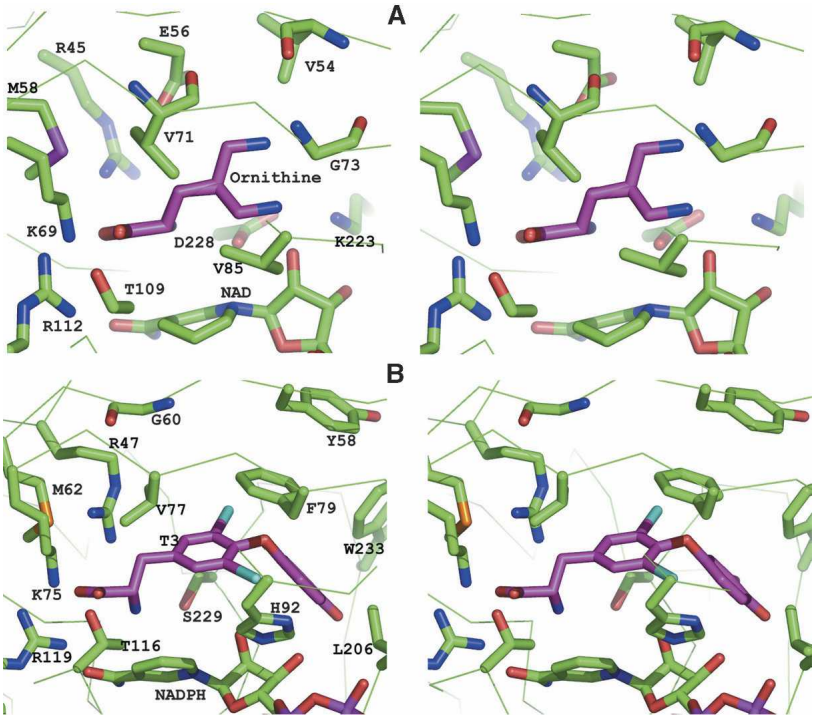

Figure 3. The ligand-binding sites comparison between *Pp*OCD and human CRYM in the similar orientation. Ornithine and T_3 are shown with carbon colored magenta, nitrogen blue, oxygen red, and iodine cyan. Protein residues are shown with carbon green, nitrogen blue, oxygen red, and sulfur orange. (*A*) The active site residues of *Pp*OCD. Residues within 4 Å of the ornithine are displayed. The ligand ornithine–CH_2–NH_2 tail has double conformations. (*B*) The proposed T_3 binding model in human CRYM.

Materials and methods

Gene cloning, expression, and protein purification

The cDNA encoding CRYM was cloned from a human brain cDNA library (Clontech) by PCR and constructed into the NdeI/XhoI-cleaved pET22b(+) (Novagen). Purified plasmid was confirmed by DNA sequencing and then used to transform competent *E. coli* BL21(DE3) cells (Stratagene). A single colony was selected and grown in Luria Broth medium with 100 μg/mL ampicillin at 37°C to A_{600} = 0.9, followed by induction with 0.5 mM isopropylthiogalactoside for 4 h. Cells were lysed in 20 mM sodium cacodylate (pH 6.5), 200 mM NaCl, and 1 mM PMSF by sonication on ice. After centrifugation, the supernatant was loaded onto a Nickel Chelating Sepharose Fast Flow column (Amersham Biosciences) for purification. Pure CRYM was pooled; dialyzed against 20 mM sodium cacodylate (pH 6.5), 50 mM NaCl, 1 mM PMSF, and 5 mM NADPH; concentrated to 10 mg /mL; and stored at −20°C.

Crystallization and data collection

Crystals of human CRYM were grown by vapor diffusion by equilibrating 1 μL of protein (10 mg/mL) mixed with 1 μL of reservoir solution against a reservoir containing 0.2 M ammonium formate, 20% polyethylene glycol 3350 with the pH value about 6.5 over a period of 4–5 d at 277 K. Crystals were soaked in reservoir liquor of the same composition but supplemented with 20% (v/v) glycerol for cryoprotection for ~1 min before freezing them for data collection. Data were collected at the home facility using a Rigaku R-AXIS IV++ imaging-plate system with a Rigaku FRE Cu rotating-anode generator in the Institute of Biochemistry and Cell Biology, Shanghai Institutes for Biological Sciences, Chinese Academy of Sciences. Data were processed by HKL2000 (Otwinowski and Minor 1997).

Structure determination and refinement

The human CRYM structure was solved by molecular replacement with Molrep in the CCP4 suite (Vagin and Teplyakov 1997) using polyala of the alanine dehydrogenase monomer (PDB ID 1OMO; ~30% sequence identity with human CYRM) as the search model. Five peaks in the rotation function yielded two solutions after the translation function search that packed well within the unit cell and, together with unbiased features in the initial electron density map, confirmed the correctness of the molecular replacement solution. The program Coot (Emsley and Cowtan 2004) was used to rebuild the initial model. The model was refined to 2.6 Å resolution using the Crystallography and NMR System (Brunger et al. 1998) with the twofold Non-Crystallographic Symmetry (NCS) as a restraint. NADPH and water molecules were added to the model, and individual atomic *B*-factors were refined in a later stage of refinement. The stereochemical qualities of the final models were checked by PROCHECK (Laskowski et al. 1993). The final refinement statistics are listed in Table 1. The coordinates and structure factors have been deposited in the Protein Data Bank (accession codes 2I99).

Table 1. *Statistics of data collection and refinement*

Data collection	
Space group	$P2_12_12_1$
Cell dimensions (Å)	a = 70.98, b = 90.86, c = 101.183
Resolution (Å)	30–2.60
Highest-resolution shell (Å)	2.69–2.60
Number of observations	124,410
Unique reflections	20,665 (2001)
Completeness (%)	99.8 (100)
R_{merge} (%)[a]	9.5 (49.4)
Refinement	
Reflections in working set	19,619
Reflections in test set	1930
R_{work}/R_{free}[b]	0.213 (0.29)/0.263 (0.34)
Mean temperature factor (Å^2)	34.3
RMSD bond lengths (Å)[c]	0.007
RMSD bond angles (°)	1.40
Ramachandran plot quality (%)	
Most favored	91.5
Additionally allowed	8.5

The numbers in parentheses represent the value for the highest-resolution shell.

[a] $R_{merge} = \sum_h\sum_i|I_{ih} - \langle I_h\rangle|/\sum_h\sum_i\langle I_h\rangle$, where $\langle I_h\rangle$ is the mean intensity of the i observations of reflection h.

[b] $R_{work} = \sum||F_{obs}| - |F_{calc}||/\sum|F_{obs}|$, where F_{obs} and F_{calc} are observed and calculated structure factors, respectively. $R_{free} = \sum_T||F_{obs}| - |F_{calc}||/\sum_T|F_{obs}|$, where T is a test data set of 10% of the total reflections randomly chosen and set aside prior to refinement.

[c] RMSD is the root mean squared deviation from ideal values.

Acknowledgments

We thank Jianping Ding in the Institute of Biochemistry and Cell Biology, Shanghai Institutes for Biological Sciences, Chinese Academy of Sciences for diffraction data collection. This work was supported by the National Foundation of Talent Youth (Grant No. 30225015), the 973 programs (No. 2004CB720008 and 2006CB0D1705), National Natural Science Foundation of China (Grant No. 10490193), Chinese Academy of Sciences (KSCX1-YW-R-61), and Shanghai Institute of Applied Physics (Grant No. 90040321).

References

Abe, S., Katagiri, T., Saito-Hisaminato, A., Usami, S., Inoue, Y., Tsunoda, T., and Nakamura, Y. 2003. Identification of CRYM as a candidate responsible for nonsyndromic deafness, through cDNA microarray analysis of human cochlear and vestibular tissues. *Am. J. Hum. Genet.* **72:** 73–82.

Beslin, A., Vie, M.P., Blondeau, J.P., and Francon, J. 1995. Identification by photoaffinity labelling of a pyridine nucleotide-dependent tri-iodothyronine-binding protein in the cytosol of cultured astroglial cells. *Biochem. J.* **305:** 729–737.

Bottoms, C.A., Smith, P.E., and Tanner, J.J. 2002. A structurally conserved water molecule in Rossmann dinucleotide-binding domains. *Protein Sci.* **11:** 2125–2137.

Brunger, A.T., Adams, P.D., Clore, G.M., DeLano, W.L., Gros, P., Grosse-Kunstleve, R.W., Jiang, J.S., Kuszewski, J., Nilges, M., Pannu, N.S., et al. 1998. Crystallography & NMR system: A new software suite for macromolecular structure determination. *Acta Crystallogr. D Biol. Crystallogr.* **54:** 905–921.

Carugo, O. and Argos, P. 1997. NADP-dependent enzymes. I: Conserved stereochemistry of cofactor binding. *Proteins* **28:** 10–28.

Chen, H., Phillips, H.A., Callen, D.F., Kim, R.Y., Wistow, G.J., and Antonarakis, S.E. 1992. Localization of the human gene for μ-crystallin to chromosome 16p. *Genomics* **14:** 1115–1116.

DeLano, W.L. 2002. *The PyMOL user's manual*. DeLano Scientific, San Carlos, CA.

Emsley, P. and Cowtan, K. 2004. Coot: Model-building tools for molecular graphics. *Acta Crystallogr. D Biol. Crystallogr.* **60:** 2126–2132.

Gallagher, D.T., Monbouquette, H.G., Schroder, I., Robinson, H., Holden, M.J., and Smith, N.N. 2004. Structure of alanine dehydrogenase from *Archaeoglobus*: Active site analysis and relation to bacterial cyclodeaminases and mammalian μ crystallin. *J. Mol. Biol.* **342:** 119–130.

Goodman, J.L., Wang, S., Alam, S., Ruzicka, F.J., Frey, P.A., and Wedekind, J.E. 2004. Ornithine cyclodeaminase: Structure, mechanism of action, and implications for the μ-crystallin family. *Biochemistry* **43:** 13883–13891.

Gouet, P., Courcelle, E., Stuart, D.I., and Metoz, F. 1999. ESPript: Analysis of multiple sequence alignments in PostScript. *Bioinformatics* **15:** 305–308.

Hashizume, K., Kobayashi, M., and Miyamoto, T. 1986. Active and inactive forms of 3,5,3′-triiodo-L-thyronine (T3)-binding protein in rat kidney cytosol: Possible role of nicotinamide adenine dinucleotide phosphate in activation of T3 binding. *Endocrinology* **119:** 710–719.

Hashizume, K., Miyamoto, T., Ichikawa, K., Yamauchi, K., Sakurai, A., Ohtsuka, H., Kobayashi, M., Nishii, Y., and Yamada, T. 1989. Evidence for the presence of two active forms of cytosolic 3,5,3′-triiodo-L-thyronine (T3)-binding protein (CTBP) in rat kidney. Specialized functions of two CTBPs in intracellular T3 translocation. *J. Biol. Chem.* **264:** 4864–4871.

Kabsch, W. and Sander, C. 1983. Dictionary of protein secondary structure: Pattern recognition of hydrogen-bonded and geometrical features. *Biopolymers* **22:** 2577–2637.

Kim, R.Y., Gasser, R., and Wistow, G.J. 1992. μ-Crystallin is a mammalian homologue of *Agrobacterium* ornithine cyclodeaminase and is expressed in human retina. *Proc. Natl. Acad. Sci.* **89:** 9292–9296.

Kohrle, J. 1999. Local activation and inactivation of thyroid hormones: The deiodinase family. *Mol. Cell. Endocrinol.* **151:** 103–119.

Langsetmo, K., Fuchs, J., and Woodward, C. 1989. *Escherichia coli* thioredoxin folds into two compact forms of different stability to urea denaturation. *Biochemistry* **28:** 3211–3220.

Laskowski, R.A., MacArthur, M.W., Moss, D.S., and Thornton, J.M. 1993. PROCHECK: A program to check the stereochemical quality of protein structures. *J. Appl. Crystallogr.* **26:** 283–291.

Mori, J., Suzuki, S., Kobayashi, M., Inagaki, T., Komatsu, A., Takeda, T., Miyamoto, T., Ichikawa, K., and Hashizume, K. 2002. Nicotinamide adenine dinucleotide phosphate-dependent cytosolic T_3 binding protein as a regulator for T_3-mediated transactivation. *Endocrinology* **143:** 1538–1544.

Ondo-Mbele, E., Vives, C., Kone, A., and Serre, L. 2005. Intriguing conformation changes associated with the *trans*/*cis* isomerization of a prolyl residue in the active site of the DsbA C33A mutant. *J. Mol. Biol.* **347:** 555–563.

Oshima, A., Suzuki, S., Takumi, Y., Hashizume, K., Abe, S., and Usami, S. 2006. CRYM mutations cause deafness through thyroid hormone binding properties in the fibrocytes of the cochlea. *J. Med. Genet.* **43:** e25.

Otwinowski, Z. and Minor, W. 1997. Processing of X-ray diffraction data collected in oscillation mode. *Methods Enzymol.* **276:** 307–326.

Rossmann, M.G., Moras, D., and Olsen, K.W. 1974. Chemical and biological evolution of nucleotide-binding protein. *Nature* **250:** 194–199.

Schroder, I., Vadas, A., Johnson, E., Lim, S., and Monbouquette, H.G. 2004. A novel archaeal alanine dehydrogenase homologous to ornithine cyclodeaminase and μ-crystallin. *J. Bacteriol.* **186:** 7680–7689.

Segovia, L., Horwitz, J., Gasser, R., and Wistow, G. 1997. Two roles for μ-crystallin: A lens structural protein in diurnal marsupials and a possible enzyme in mammalian retinas. *Mol. Vis.* **3:** 9.

Thompson, J.D., Higgins, D.G., and Gibson, T.J. 1994. CLUSTAL W: Improving the sensitivity of progressive multiple sequence alignment through sequence weighting, position-specific gap penalties and weight matrix choice. *Nucleic Acids Res.* **22:** 4673–4680.

Truckses, D.M., Somoza, J.R., Prehoda, K.E., Miller, S.C., and Markley, J.L. 1996. Coupling between *trans*/*cis* proline isomerization and protein stability in staphylococcal nuclease. *Protein Sci.* **5:** 1907–1916.

Vagin, A. and Teplyakov, A. 1997. MOLREP: An automated program for molecular replacement. *J. Appl. Crystallogr.* **30:** 1022–1025.

Vie, M.P., Evrard, C., Osty, J., Breton-Gilet, A., Blanchet, P., Pomerance, M., Rouget, P., Francon, J., and Blondeau, J.P. 1997. Purification, molecular cloning, and functional expression of the human nicodinamide–adenine dinucleotide phosphate-regulated thyroid hormone-binding protein. *Mol. Endocrinol.* **11:** 1728–1736.

Wallace, A.C., Laskowski, R.A., and Thornton, J.M. 1995. LIGPLOT: A program to generate schematic diagrams of protein–ligand interactions. *Protein Eng.* **8:** 127–134.

Wistow, G. and Kim, H. 1991. Lens protein expression in mammals: Taxon-specificity and the recruitment of crystallins. *J. Mol. Evol.* **32:** 262–269.

Yen, P.M. 2001. Physiological and molecular basis of thyroid hormone action. *Physiol. Rev.* **81:** 1097–1142.

Zhang, J. and Lazar, M.A. 2000. The mechanism of action of thyroid hormones. *Annu. Rev. Physiol.* **62:** 439–466.